

Supplemental Information

Supplemental Data

Table S1. Numbers of individuals sequenced from each of three major refugia for 12 gallwasp and 19 chalcidoid parasitoid species, the generation time of each species (g) and the mitochondrial locus and sequence length used. π_{net} , the net pairwise divergence between two populations for each species (see Supplemental Experimental Procedures), is the most informative summary statistic used in the msBayes analysis. For each species we provide the rank and π_{net} value for each pair of refugia, with the expectation that species with lower ranked π_{net} values were involved in more recent divergence events. Samples marked n/a refer to species absent from a region. Though present in Iberia, no samples of *Cynips quercusfolii* were available. Host richness is the total number of gall species and generations attacked by each parasitoid species, with ? indicating taxa for which data are lacking (in the case of *M. dorsalis* due to recent demonstration of two cryptic taxa [25]). Genbank accession numbers for each species will be added upon acceptance of the manuscript.]

Species	Guild and parasitoid family	Host richness rank/total	g	locus	Genbank Accession Nos.	Seq. length (bp)	Sample size				π_{net} (rank/value)	
							Iran	Balkan	Iberia	Total	Balkans/Iberia	Iran/Balkans
<i>Andricus curvator</i>	Gallwasp		0.5	<i>cytb</i>	JQ416309-35	433	n/a	16	11	27	5/0.00782	n/a
<i>Andricus inflator</i>	Gallwasp		0.5	<i>cytb</i>	JQ416336-43	433	4	2	2	8	3/0.00690	7/0.05110
<i>Andricus kollari</i>	Gallwasp		0.5	<i>cytb</i>	See footnote 1	433	n/a	14	15	29	7/0.01810	n/a
<i>Andricus lucidus</i>	Gallwasp		0.5	<i>cytb</i>	AJ228464, JQ416344-57	433	5	10	n/a	15	n/a	6/0.01978
<i>Andricus quercusramuli</i>	Gallwasp		0.5	<i>cytb</i>	JQ416358-97	433	n/a	20	20	40	8/0.02399	n/a
<i>Andricus quercustozæ</i>	Gallwasp		0.5	<i>cytb</i>	See footnote 2	433	19	9	33	61	10/0.02939	9/0.06131
<i>Andricus coriarius</i>	Gallwasp		0.5	<i>cytb</i>	See footnote 3	433	14	10	5	29	2/0.00281	1/0.00894
<i>Andricus grossulariæ</i>	Gallwasp		0.5	<i>cytb</i>	JQ416398-417	433	8	2	10	20	1/0.00000	5/0.01937
<i>Biorhiza pallida</i>	Gallwasp		0.5	<i>cytb</i>	See footnote 4	433	2	16	22	40	6/0.00822	4/0.01693
<i>Cynips quercus</i>	Gallwasp		0.5	<i>cytb</i>	JQ416435-78	433	14	19	11	44	9/0.02838	8/0.05141
<i>Cynips quercusfolii</i>	Gallwasp		0.5	<i>cytb</i>	JQ416479-500	433	14	8	0	22	n/a	3/0.01242
<i>Neuroterus quercusbaccarum</i>	Gallwasp		0.5	<i>cytb</i>	JQ416501-46	433	15	12	19	46	4/0.00763	2/0.01157
<i>Aprostocetus cerricola</i>	Eulophidae	13/15	0.5	<i>COI</i>	JQ416723-31	698	3	6	n/a	9	n/a	10/0.01062
<i>Aulogynnis gallarum</i>	Eulophidae	7/46	0.5	<i>COI</i>	JQ416732-63	698	9	12	11	32	5/0.00193	11/0.01744
<i>Baryscapus pallidæ</i>	Eulophidae	12/19	0.5	<i>COI</i>	JQ416764-96	698	7	21	5	33	11/0.01096	1/0.00074
<i>Eupelmus nubilipennis</i> (=E. annulatus)	Eupelmidae	?	0.5	<i>COI</i>	JQ416968-81	656	4	6	4	14	10/0.00779	7/0.00819
<i>Eupelmus urozonus</i>	Eupelmidae	3/87	0.5	<i>COI</i>	JQ416942-67	655	6	11	9	26	12/0.01098	6/0.00630
<i>Eurytoma brunniiventris</i>	Eurytomidae	1/100	0.5	<i>cytb</i>	JQ416547-623	433	15	37	25	77	7/0.00333	8/0.00993
<i>Eurytoma adleriæ</i>	Eurytomidae	?	0.5	<i>cytb</i>	JQ416624-722	433	17	65	17	99	15/0.02335	14/0.01999
<i>Cecidostiba fingsosæ</i>	Pteromalidae	4/65	0.5	<i>COI</i>	JQ416982-7026	652	21	16	8	45	8/0.00366	9/0.00987
<i>Hobbya stenonota</i>	Pteromalidae	11/31	0.5	<i>COI</i>	JQ416797-814	698	6	9	3	18	13/0.01245	15/0.02711

<i>Mesopolobus fasciventris</i>	Pteromalidae	6/47	0.33		JQ416815-8							
<i>Mesopolobus xanthocerus</i>	Pteromalidae	8/37	1	<i>COI</i>	JQ416819-42	698	n/a	2	2	4	3/0.00000	n/a
<i>Ormyrus nitidulus</i>	Ormyridae	5/52	0.5	<i>cytb</i>	JQ417027-107	745	28	31	22	81	17/0.06629	n/a
<i>Ormyrus pomaceus</i>	Ormyridae	2/95	0.5	<i>COI</i>	JQ416843-72	698	13	8	9	30	14/0.01460	16/0.04659
<i>Megastigmus dorsalis</i> sp1	Torymidae	?	0.5	<i>cytb</i>	See footnote 5	433	21	33	22	76	18/0.08897	5/0.00412
<i>Megastigmus dorsalis</i> sp2	Torymidae	?	0.5	<i>cytb</i>	See footnote 6	433	3	2	2	7	6/0.00312	12/0.01774
<i>Megastigmus stigmatizans</i>	Torymidae	14/14	1	<i>cytb</i>	See footnote 7	590	31	20	40	91	2/0.00000	13/0.01905
<i>Torymus auratus</i>	Torymidae	9/37	0.5	<i>COI</i>	JQ416873-95	698	5	9	9	23	9/0.00502	3/0.00295
<i>Torymus cyaneus</i>	Torymidae	15/7	1	<i>COI</i>	JQ416896-917	698	6	11	5	22	1/0.00000	2/0.00261
<i>Torymus flavipes</i>	Torymidae	10/34	0.5	<i>COI</i>	JQ416918-41	698	n/a	16	8	24	16/0.06364	4/0.00400
Total 31 species						290		468	358	1116	4/0.00012	n/a

1. *Andricus kollari*: AF242739-40, AF242746, AF242765-66, EF031340-41, EF031344, EF031359-60, EF031368-69, EF031375, EF031377-80, EF031385-87, EF031391, EF031408-09, EF031411, EF031418, EF031422-24, EF031437

2. *Andricus quercustozae*: AJ228467, AY157269-70, AY157272, AY157286-88, AY157296, JQ228941-48, JQ228950-57, JQ228976, JQ228979-82, JQ228993-JQ229002

3. *Andricus coriarius*: AF539556-57, AJ228458, EF029996-97, EF029999-EF030003, EF030012, EF030021-25

4. *Biorhiza pallida*: AF339616-18, AF339620-21, AF339623-28, JQ416418-34

5. *Megastigmus dorsalis* species 1: GU123486-87, GU123489-91, GU123500-02, GU123512-13, GU123525-26, GU123530-33, GU123535, GU123538-46, GU123548, GU123572-73

6. *Megastigmus dorsalis* species 2: GU123528, GU123536-37, GU123547, GU123567-68

7. *Megastigmus stigmatizans*: FJ026675, FJ026677, FJ026679-80, FJ026682, FJ026684-88, FJ026698, FJ026703, FJ026709-11, FJ026714, FJ026716-17, FJ026724, FJ026726-27

Table S2. (A) Per site divergence for pairs of individuals sampled from neighbouring refugia (Iran/Balkans and Balkans/Iberia) for *COI* and *cytb* for 11 gallwasp and 16 parasitoid species. Differences between loci are non-significant for either pair of refugia (see Supplemental Experimental Procedures). Data are missing for 1 gallwasp (*Andricus quercusramuli*) and three parasitoids (*Eurytoma brunniventris*, *E. adleriae* and *Mesopolobus fasciiventris*). n/a refers to comparisons in which one refugium falls outside the species range or to cases where the comparison could not be made due to PCR or sequencing failure. (B) Genbank accession numbers for each species and region.

A

Species	<i>cytb</i>			<i>COI</i>		
	Length (bp)	Iran/Balkan	Balkan/Iberia	Length (bp)	Iran/Balkan	Balkan/Iberia
Gallwasps						
<i>Andricus coriarius</i>	433	0.025	0.021	658	0.030	0.030
<i>Andricus curvator</i>	433	n/a	0.055	658	n/a	0.052
<i>Andricus grossulariae</i>	433	0.099	0.007	658	0.123	0.009
<i>Andricus inflator</i>	433	0.060	n/a	658	0.074	n/a
<i>Andricus kollari</i>	433	n/a	0.035	658	n/a	0.017
<i>Andricus lucidus</i>	433	0.025	n/a	658	0.032	n/a
<i>Andricus quercustozae</i>	433	0.048	0.030	658	0.033	0.026
<i>Biorhiza pallida</i>	433	n/a	0.028	658	n/a	0.014
<i>Cynips quercus</i>	433	0.074	0.039	658	0.064	0.047
<i>Cynips quercusfolii</i>	433	0.018	n/a	658	0.024	n/a
<i>Neuroterus quercusbaccarum</i>	433	0.016	0.016	658	0.021	0.012
Parasitoids						
<i>Aprostocetus cerricola</i>	433	0.007	n/a	698	0.009	n/a
<i>Aulogymnus gallarum</i>	433	0.058	0.005	698	0.042	0.006
<i>Baryscapus pallidae</i>	433	0.016	0.055	698	0.010	0.069
<i>Cecidostiba fungosa</i>	433	0.018	0.007	652	0.031	0.003
<i>Eupelmus nubilipennis</i>	433	0.032	0.023	656	0.030	0.030
<i>Eupelmus urozonus</i>	433	0.018	0.016	655	0.026	0.027
<i>Hobbya stenonota</i>	433	0.018	0.009	698	0.033	0.020
<i>Megastigmus dorsalis sp1</i>	433	0.023	0.002	655	0.011	0.003
<i>Megastigmus dorsalis sp2</i>	433	0.032	0.005	698	0.016	0
<i>Megastigmus stigmatizans</i>	590	0.003	0.007	698	0.003	0.006
<i>Mesopolobus xanthocerus</i>	433	n/a	0.055	698	n/a	0.072
<i>Ormyrus nitidulus</i>	745	0.064	0.034	654	0.049	0.029
<i>Ormyrus pomaceus</i>	433	0.014	0.088	698	0.027	0.097
<i>Torymus auratus</i>	760	0.012	0.008	698	0.007	0.006
<i>Torymus cyaneus</i>	433	0.035	0.106	698	0.020	0.079
<i>Torymus flavipes</i>	433	n/a	0	698	n/a	0.003
Mean		0.033	0.028		0.033	0.029

B

Species	<i>cytb</i>			<i>COI</i>		
	Iran	Balkans	Iberia	Iran	Balkans	Iberia
Gallwasps						
<i>Andricus coriarius</i>	JQ417180	JQ417182	JQ417181	JQ417108	JQ417110	JQ417109
<i>Andricus curvator</i>		JQ416328	JQ416310		JQ417112	JQ417111
<i>Andricus grossulariae</i>	JQ416401	JQ416406	JQ416408	JQ417115	JQ417114	JQ417113
<i>Andricus inflator</i>	JQ416338	JQ416342	JQ416337		JQ417117	JQ417116
<i>Andricus kollari</i>		EF031418	EF031359		JQ417119	JQ417118
<i>Andricus lucidus</i>	JQ416344	JQ416354		JQ417120	JQ417121	
<i>Andricus quercustozae</i>	JQ228952	JQ228976	JQ229002	JQ417124	JQ417123	JQ417122
<i>Biorhiza pallida</i>		JQ416418	JQ416429	JQ417125	JQ417126	
<i>Cynips quercus</i>	JQ416447	JQ416477	JQ416437	JQ417127	JQ417128	JQ417129
<i>Cynips quercusfolii</i>	JQ416481	JQ416498		JQ417130	JQ417131	
<i>Neuroterus quercusbaccarum</i>	JQ416506	JQ416521	JQ416545	JQ417132	JQ417134	JQ417133
Parasitoids						
<i>Aprostocetus cerricola</i>	JQ417147	JQ417148		JQ416725	JQ416729	
<i>Aulogymnus gallarum</i>	JQ417151	JQ417149	JQ417150	JQ416735	JQ416750	JQ416757
<i>Baryscapus pallidae</i>	JQ417153	JQ417152	JQ417154	JQ416765	JQ416786	JQ416794
<i>Cecidostiba fungosa</i>	JQ417157	JQ417155	JQ417156	JQ416996	JQ417012	JQ417024
<i>Eupelmus nubilipennis</i>	JQ417159	JQ417158	JQ417160	JQ416970	JQ416972	JQ416980
<i>Eupelmus urozonus</i>	JQ417162	JQ417161	JQ417163	JQ416945	JQ416950	JQ416965
<i>Hobhya stenonota</i>	JQ417165	JQ417164	JQ417166	JQ416800	JQ416803	JQ416812
<i>Megastigmus dorsalis sp1</i>	GU123535	GU123532	GU123487	JQ417140	JQ417139	JQ417138
<i>Megastigmus dorsalis sp2</i>	GU123536	GU123567	GU123528	JQ417137	JQ417136	JQ417135
<i>Megastigmus stigmatizans</i>	FJ026675	FJ026679	FJ026711	JQ417143	JQ417142	JQ417141
<i>Mesopolobus xanthocerus</i>	JQ417167	JQ417168		JQ416826	JQ416837	
<i>Ormyrus nitidulus</i>	JQ417082	JQ417031	JQ417099	JQ417146	JQ417145	JQ417144
<i>Ormyrus pomaceus</i>	JQ417169	JQ417170	JQ417171	JQ416847	JQ416857	JQ416865
<i>Torymus auratus</i>	JQ417177	JQ417178	JQ417179	JQ416873	JQ416885	JQ416893
<i>Torymus cyaneus</i>	JQ417174	JQ417172	JQ417173	JQ416896	JQ416902	JQ416915
<i>Torymus flavipes</i>	JQ417175	JQ417176		JQ416919	JQ416941	

Table S3. Accuracy and error rate appraisals of (A) Approximate Bayes Factor (BF)-based model selection, and (B) posterior mode for Ψ , the number of pairwise divergence pulses, using simulation validation on pseudo-observed data sets (PODS). For each set of appraisals, posterior mode estimates and Bayes Factors were calculated on each of 100 PODS whose parameters were randomly drawn from the prior, with Ψ drawn from a discrete uniform distribution or fixed at 1 (a single pulse; $\Psi = 1$). The PODS matched the 18 species pairs of Balkan/Iberian parasitoids with respect to sample configuration and number of base pairs. “BF correct” refers to Bayes Factor-based selection of the correct model at two of the threshold values proposed by Jeffries (3 for moderate support, and 10 for strong support) [45]. “BF error” refers to Bayes Factor-based rejection of the correct model. It is assumed that $\text{Var}(\tau)/E(\tau) < 0.01$ is consistent with a single pulse of co-divergence ($\Psi = 1$).

(A)	Ψ	$\text{Var}(\tau)/E(\tau)$
<i>Bayes Factor Threshold for model choice = 3</i>		
Pr(BF correct true $\Psi > 1$)	0.93	0.89
Pr(BF error true $\Psi > 1$)	0.00	0.00
Pr(BF correct true $\Psi = 1$)	0.46	0.67
Pr(BF error true $\Psi = 1$)	0.04	0.07
Pr(BF correct true $\Psi > 3$)	0.79	N/A
Pr(BF error true $\Psi > 3$)	0.04	N/A
<i>Bayes Factor Threshold for model choice = 10</i>		
Pr(BF correct true $\Psi > 1$)	0.88	0.83
Pr(BF error true $\Psi > 1$)	0.00	0.00
Pr(BF correct true $\Psi = 1$)	0.44	0.57
Pr(BF error true $\Psi = 1$)	0.02	0.06
Pr(BF correct true $\Psi > 3$)	0.73	N/A
Pr(BF error true $\Psi > 3$)	0.04	N/A
(B)		
Pr(Mode estimate correct true $\Psi > 1$)	1.00	1.00
Pr(Mode estimate error true $\Psi > 1$)	0.00	0.00
Pr(Mode estimate correct true $\Psi = 1$)	0.91	0.96
Pr(Mode estimate error true $\Psi = 1$)	0.09	0.04
Pr(Mode estimate correct true $\Psi > 3$)	0.96	N/A
Pr(Mode estimate error true $\Psi > 3$)	0.04	N/A

Figure S1. Posterior probability distributions for ω , the ratio of variance to the mean in species divergence times among population pairs, $\text{Var}(\tau)/E(\tau)$, for each pair of refugia and guild (see Supplemental Experimental Procedures). (A), (B) show results for the herbivorous gallwasp guild, and (C), (D) show results for the parasitoid guild. Clustering of values near $\omega = 0$ indicates support for a single divergence event (for gallwasps in Balkans/Iberia, and parasitoids in Asia/Balkans), while non-zero values support multiple divergence events (for gallwasps in Asia/Balkans and parasitoids in Balkans/Iberia). Results for this parameter are wholly concordant with those for the posterior distribution of Ψ .

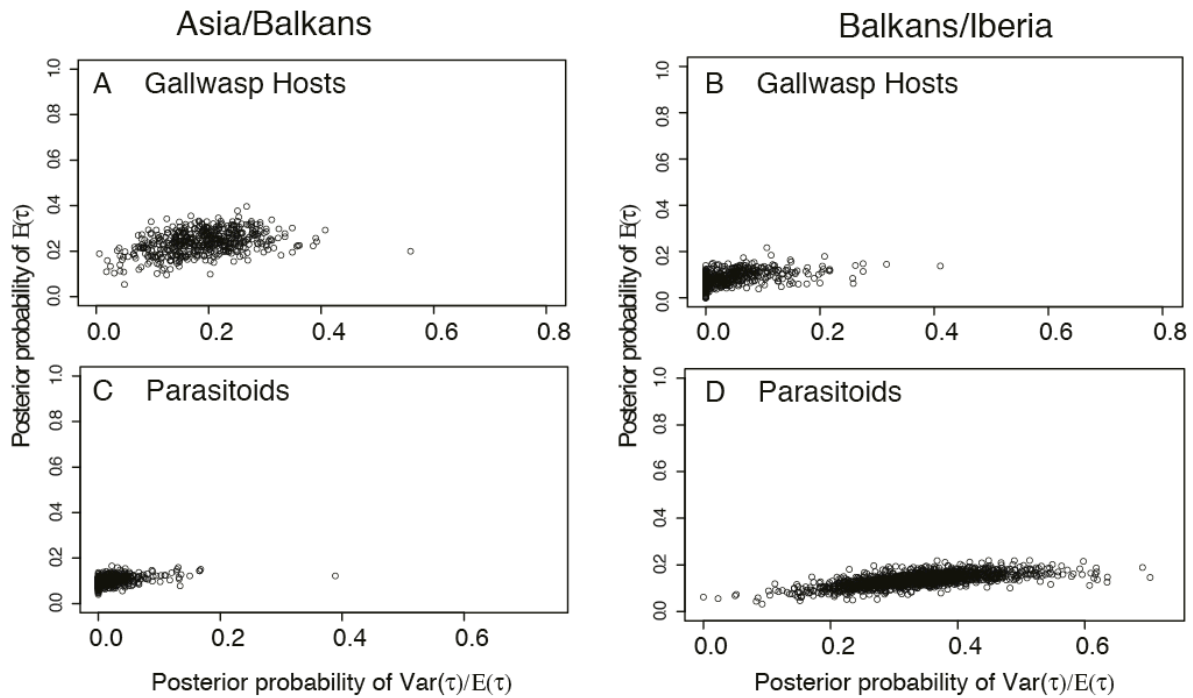


Figure S2. Tests of species assignment to divergence events, and robustness of patterns to uncertainty in Ψ . (A) and (B) show allocation of species to specific divergence events given the most strongly supported value of Ψ . In both (A) and (B), solid lines show results obtained when taxon membership of divergence pulses is unconstrained, while dashed lines show results obtained when the same number of species was allocated to each event on the basis of their ranking for π_{net} (see Supplemental Experimental Procedures and Table S1). (A) Dispersal between Asia and the Balkans. (B) Dispersal between the Balkans and Iberia. Note there is no dotted line for the gallwasps in Balkans/Iberia, or the parasitoids in Iran/Balkans, because only a single event was inferred. Panels (C) through (J) show robustness of inferred patterns to variation in Ψ from 2-5 pulses. In each panel, Ψ is constrained to the specific value shown (2, 3, 4, or 5 pulses). For Balkans/Iberia divergence (panels C-F), at least one parasitoid pulse always predates the gallwasps, and at least one always postdates them. For Asia/Balkans divergence (panels G-J), the single parasitoid divergence pulse always postdates at least one gallwasp pulse.

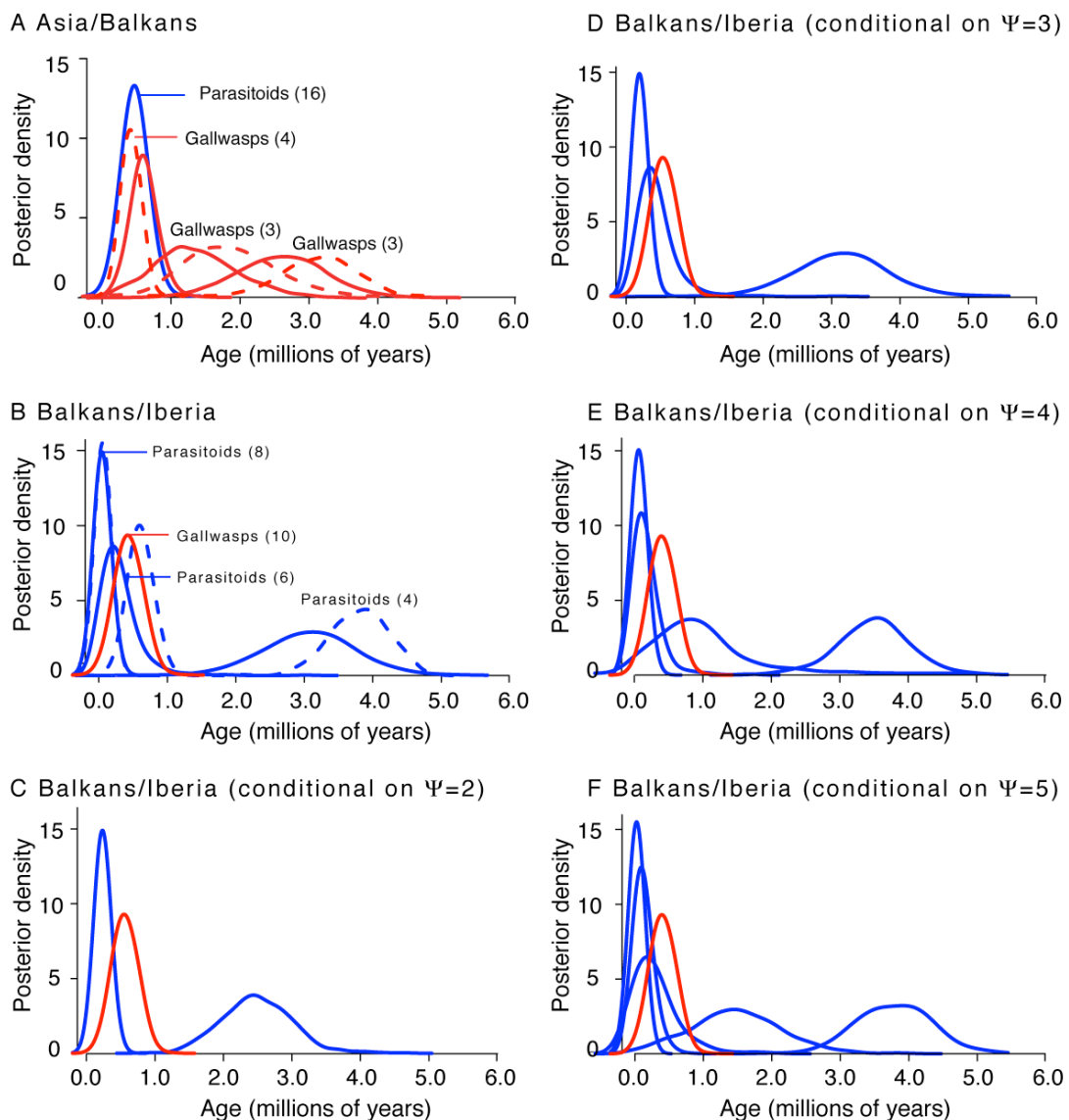


Figure S2 (continued)

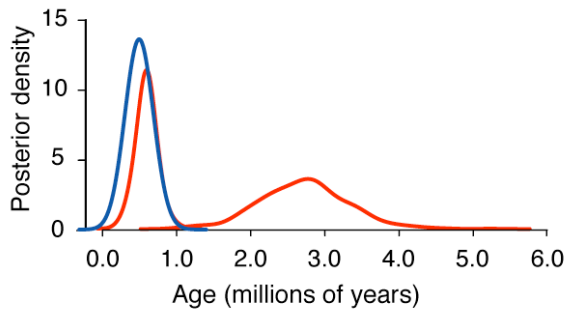
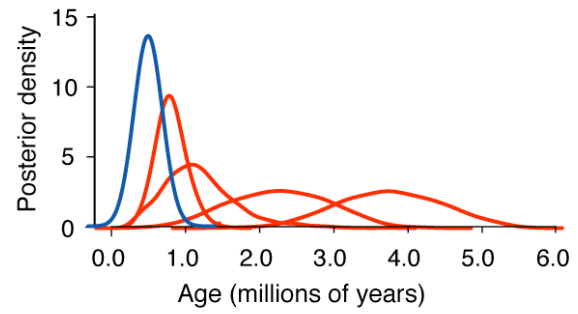
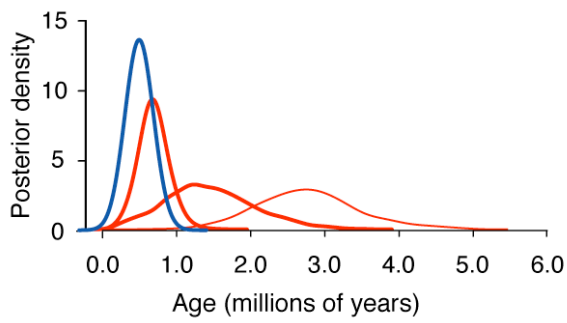
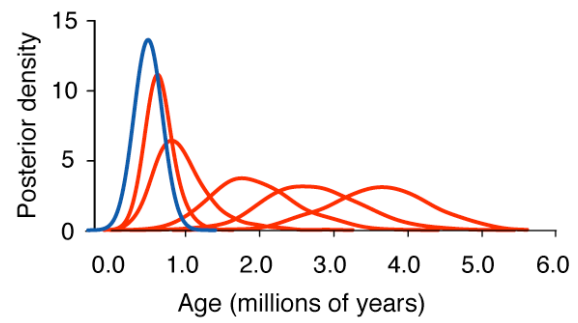
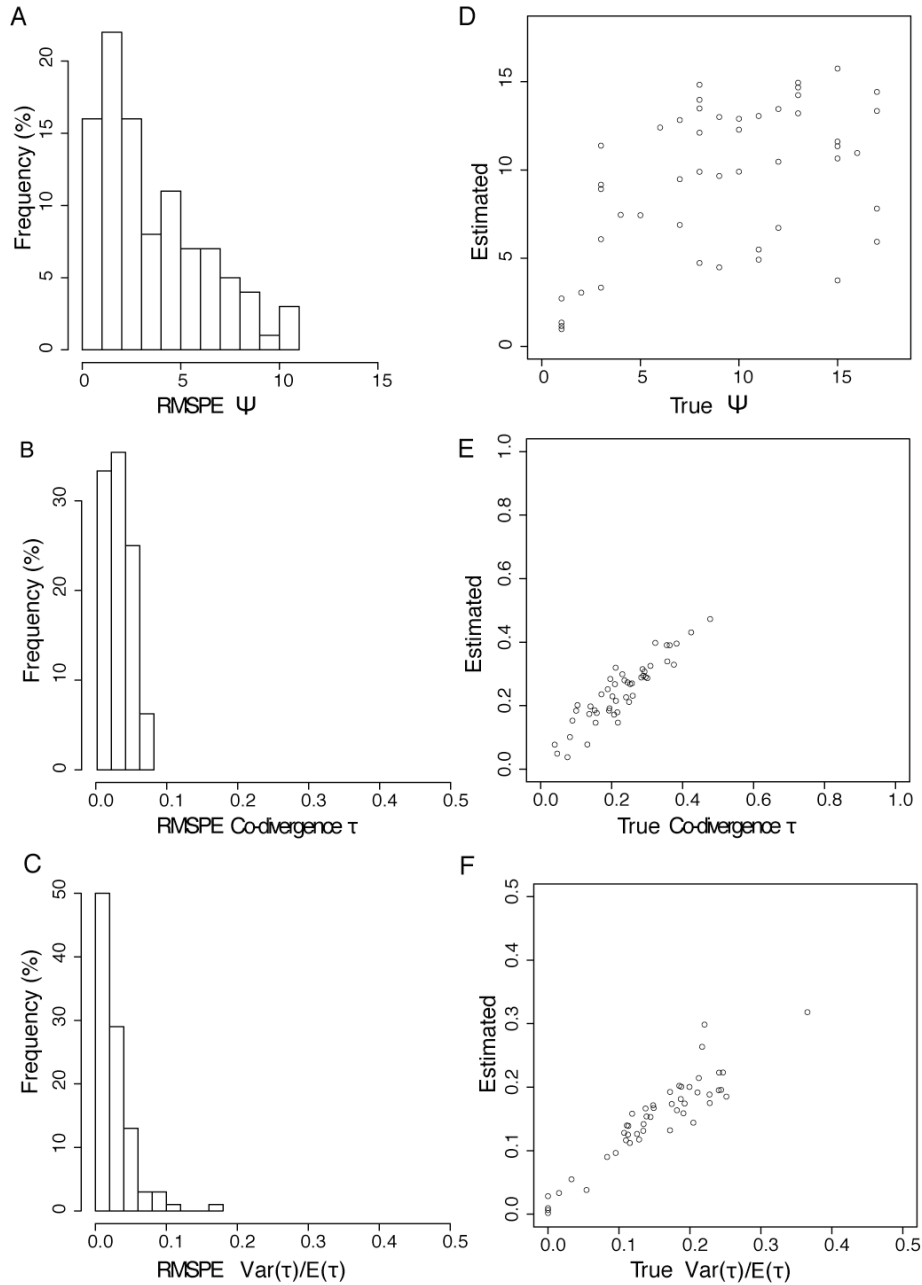
G Asia/Balkans (conditional on $\Psi=2$)I Asia/Balkans (conditional on $\Psi=4$)H Asia/Balkans (conditional on $\Psi=3$)J Asia/Balkans (conditional on $\Psi=5$)

Figure S3. Empirical validation of estimation procedures for τ , shared Ψ and $\text{Var}(\tau)/E(\tau)$. (A), (B), (C) Frequency distributions of the Root Mean Square Posterior Error (RMSPE) across 50 mode estimates of τ , shared Ψ and $\text{Var}(\tau)/E(\tau)$ given 50 pseudo-observed data sets (PODS) with corresponding hyperparameter values randomly drawn from the hyperprior. Each of the 50 RMSPE's are calculated as the root mean square error between each true hyperparameter value and its corresponding 1,000 accepted and transformed hyperparameter values that approximate the hyper-posterior used for estimation (out of a total 3,000,000 draws from the hyper-prior). (D), (E), (F) Mode estimates of τ , shared Ψ , and $\text{Var}(\tau)/E(\tau)$ respectively from PODS plotted against their true values randomly drawn from the hyperprior.



Supplemental Experimental Procedures

1. Estimating the number and age of multispecies co- divergence pulses

The Hierarchical Approximate Bayesian (HABC) method implemented in msBayes (described in detail elsewhere [7,29,42]) estimates the congruence in divergence times across multiple co-distributed species. Congruence is captured through 3 hyperparameters - the number (Ψ) and relative ages (τ_1, \dots, τ_w) of multispecies population divergence times between population pairs (here between neighbouring refugia) and the overall variability in divergence times scaled by the mean divergence time ($\text{Var}(\tau)/E(\tau)$). Summary statistics are used to compare observed patterns in sequence diversity with data simulated under a model of ancestral populations splitting into two daughter populations (without subsequent migration). In short, each simulation run involves (i) drawing a random value of Ψ from its discrete uniform hyperprior distribution; (ii) drawing divergence times τ, \dots, τ_n for each of the n species-pairs conditional on this instance of Ψ (i.e. all species will have the same τ if $\Psi=1$), (iii) drawing species-specific demographic parameters independently from shared prior distributions; (iv) simulating multispecies data given the randomly drawn hyperparameters as well as sample sizes, fragment lengths and known generation times for each species and (v) generating vectors of summary statistics from these simulated data sets.

Posterior distributions for the hyperparameters of interest – particularly Ψ , shared τ , and $\text{Var}(\tau)/E(\tau)$ - are generated by first applying a rejection step using the Euclidian distance between vectors of observed and simulated summary statistics, followed by either

of two methods of post-rejection adjustment. For continuous hyperparameters (shared τ , and $\text{Var}(\tau)/E(\tau)$) this involved using weighted local linear regression [39]. For discrete hyper-parameters (Ψ) this included using a feed forward neural network [45] on the
 25 retained hyperparameter sets and associated summary statistic vectors to reduce the dimensionality inherent when using multiple summary statistics in ABC [46]. Both methods were tested and empirically validated by simulating pseudo-observed data sets (PODS) with hyperparameter values that are known and drawn from their hyper-prior [27].

30 Population divergence times (τ_i) of each species were scaled relative to its effective population size (N_i), i.e. $t = \tau_i 2N_i g$, where g is the generation time in years [28]. To be able to report divergence times across co-diverging species in global coalescent time units (i.e. τ scaled by N generations) given that each species has different values of N_i , each τ_i was rescaled to the same global scale using the relationship $\tau = \tau_i \theta_i / b$, where b is the global
 35 scalar of θ . For example, if a population pair happens to have a small N_i and large τ_i (in units of $2 N_i g$), its globally expressed divergence time τ will be directly comparable to a population pair with an equal divergence in absolute time but with differing N_i (and hence differing τ_i).

40 We used four summary statistic classes calculated across all species pairs that have previously been shown to capture information about co-divergence using simulations [29]: average pairwise diversity (π), average net diversity between populations (π_{net}), Watterson's theta (θ_w) and Tajima's D (D). To allow this vector of summary statistics to

be order-independent [29] we used the ranking scheme of Huang et al (2011) [47].

45

2. Sensitivity and power analyses, and prior choices

We assumed uniform prior distributions for all species-level parameters [7,48]. The hyperprior for the hyperparameter Ψ was discrete uniform and upwardly bound by n , the number of species-pairs in any particular analysis; $\Psi = (1, n)$. Scaled effective population sizes for both ancestral populations (θ_a) and descendent pairs of daughter populations (θ_1 and θ_2) were allowed to vary independently. Given the potential sensitivity of divergence time estimates to the prior assumptions about ancestral population size (θ_a), we considered three upper prior bounds of this parameter: 0.0125, 0.025, and 0.05, where $\theta_a = 4N_a\mu g$, N_a is the species-specific effective ancestral population size, g the generation time of each species (in years) and μ is the mutation rate per site per million years. Assuming $\mu=1.15\%$ [44] and $g = 0.5$ (as is the case for most of the sample species, Table S1), these three values of θ_a correspond approximately to N_a values of 0.25, 0.5 and 1 million females respectively. We ran 3 million simulation replicates of multi-species histories under each upper prior bound for θ_a to investigate robustness of inferences.

60

For the Iran-Balkan comparison, the inferences of three co-divergence pulses in gallwasps and a single co-divergence pulse in parasitoids were robust to upper prior bounds of θ_a of 0.125, 0.25 and 0.5 and pairwise Bayes factors of ranging from 10.87 to infinity (comparing 0.25 and 0.125) and 5.15 to 20.13 (comparing 0.25 and 0.5) showed the strongest support for the intermediate upper prior bound of 0.25, which was kept in all

65

subsequent analyses. Likewise, multiple pulses of co-divergence in the Balkan-Iberia comparison for parasitoids were robust to prior upper bounds in θ_a and pairwise Bayes factors of 111.15 to 24.84 and 37.77 likewise gave strongest support for a upper prior bound of 0.25. Given the uncertainty in mitochondrial mutation rate estimates, our
70 motivation here was to investigate a plausible range of effective population sizes rather than assume any particular value. For all calculations of Bayes Factors (BF), we use the ABC approximation of BF $(M_1, M_2) = Pr(M_1/\mathbf{D})/Pr(M_2/\mathbf{D})/Pr(M_1)/Pr(M_2)$, where \mathbf{D} is the set of 1,000 summary statistic vectors passing the final ABC filter thereby approximating the posterior [39]. For using BF to choose between different pulse scenarios, we use the
75 Jeffries scale [43] in which a Bayes factor of 3 indicates moderate support for the preferred model, and a BF of 10 indicates strong support.

To validate posterior mode estimates of the hyperparameters Ψ , $\text{Var}(\tau)/E(\tau)$ and shared τ as well as to quantify approximate Bayes Factor error rates [49], we ran the
80 estimator procedure and calculated Bayes Factors on simulated data sets (PODS; pseudo-observed data sets) with known hyperparameter values that were randomly drawn from their respective hyperprior distributions (with sample sizes and hyperprior settings identical to the parasitoid data set involving 18 Balkans/Iberia species pairs). To quantify the accuracy and bias of our estimators of Ψ , $\text{Var}(\tau)/E(\tau)$ and shared τ , we first report root
85 mean square posterior error (RMSPE) [47] (see Fig. S3) and precision and accuracy of posterior mode estimates (Table S3). After exploring six different post-rejection adjustment methods for estimating Ψ , $\text{Var}(\tau)/E(\tau)$ and shared τ , we found weighted local

linear regression to work best for $\text{Var}(\tau)/E(\tau)$ and shared τ [37], and a two-step procedure involving feed forward neural networks [45] to work best for estimating Ψ . In this latter method, an initial rejection step obtaining 10,000 out of 3 million simulated draws from the hyper-prior is followed by using the feed forward neural networks [45] on this 10,000 to further retain the 1,000 draws from the hyperposterior of Ψ .

To quantify our ability to distinguish different numbers of dispersal pulses, we calculated approximate Bayes Factor (BF) error rates [49] and posterior mode estimates on each of 100 PODS where Ψ was randomly drawn from its discrete uniform distribution (1 to 18 matching the Balkans/Iberian parasitoids) or fixed at 1 (a single pulse; $\Psi = 1$). These BF error rates were quantified by reporting the probability of BF-based inference of the correct or incorrect model given that the true model is $\Psi = 1$, $\Psi > 1$, or $\Psi > 3$ (using the Jeffries BF thresholds of 3 and 10). In all three cases we used post-weighting ABC posterior estimates of Ψ as well as using adjusted ABC posterior estimates of $\text{Var}(\tau)/E(\tau)$ in the cases of $\Psi = 1$ and $\Psi > 1$ (where a single pulse is considered consistent with $\text{Var}(\tau)/E(\tau) > 0.01$). To further quantify our ability to distinguish different numbers of dispersal pulses we calculated the probability of correct and incorrect model choice using ABC posterior mode estimates of Ψ and $\text{Var}(\tau)/E(\tau)$ given that the true model is $\Psi = 1$, $\Psi > 1$, or $\Psi > 3$.

The results of these analyses are summarised in Table S3. For both significance

threshold values, when $\Psi > 1$ Bayes factors make the correct inference with high probability
110 (0.88-0.93), and never incorrectly support a single divergence event model. Similarly, when
 $\Psi = 1$ there is very rarely significant BF support for multiple pulses (0.02-0.04) (Table S3A).
Bayes factor-based inference of modal values of Ψ also has high power for both thresholds
(Table S3B). The same patterns hold for $\text{Var}(\tau)/E(\tau)$ (Table S3). Given the very strong BF
support for inference of either $\Psi = 1$ or $\Psi > 1$ in our datasets (see main text Fig.1), we
115 consider the inferences in our analysis to be robust.

3. Post-hoc allocation of taxa to divergence pulses

To confirm estimates of the number of species involved in each of $n > 1$ divergence
pulses, we used msBayes to test for simultaneous isolation in taxa assigned to pulses based
120 on net pairwise divergence values for species population pairs (π_{net} ; see 1. above, and Fig.
S2). In each analysis we simulated 3 million replicates per multi-species data set and prior
set, and constructed hyper-posterior distributions from the 500-1000 simulations closest to
the observed data with respect to four summary statistic classes described in 1. above.
Though differing in detail, there is close correspondence between the two sets of results
125 (Fig. S2).

4. Sensitivity of inferred patterns to uncertainty in Ψ

Where multiple divergence pulses are inferred, our conclusions are robust to
uncertainty in the precise number of events. This is illustrated for parasitoid and gallwasp
130 divergence between Iberia and the Balkans in Fig.S2, panels C-F. The strongly supported

modal estimate of Ψ for parasitoids for this pair of refugia is 3 (Fig.S2 B), resulting in one set of parasitoids with divergence dates younger than those for gallwasps (compatible with host tracking), and a second set of parasitoids with divergence dates older than those for gallwasps (compatible with ecological sorting). The same pattern in relative ages of divergence pulses in the two trophic groups – and hence the same inferred ecological processes - are supported for all values of Ψ from 2-5 (Fig. S2 C-F). Similarly, for gallwasp divergence between Asia and the Balkans, enemy escape from the single parasitoid pulse is inferred for at least one gallwasp pulse for all values of Ψ from 2-5 (Fig. S2 G-J).

140 5. Sequencing of mitochondrial genes, and comparison of substitution rates in *cytb* and *COI* and molecular clock calibration

Our analyses incorporate phylogeographic datasets that for each species comprise sequences either for cytochrome b (*cytb*) or cytochrome oxidase c subunit 1 (*COI*). Which of *cytb* or *COI* was used in each species was dictated in part by existing data, and in part by the ease with which new sequences could be generated. New sequences were generated by DNA extraction, PCR amplification and direct Sanger sequencing from individual wasps using published protocols and primers [23-26]. Genbank accession numbers are provided in Table S1.

Our HABC msBayes analyses assume that the per site mutation rate is constant both across species and across the two gene fragments used. However, it is possible that selective constraints could differ between genes, resulting in different net substitution rates that could confound differences in divergence estimates between the gallwasp and

parasitoid guilds as *cytb* was used for all gallwasps and *COI* for most parasitoids (Table S1). To rule out this possibility, we carried out a simple initial test: *COI* and *cytb* were
 155 sequenced from a single individual per population for as many of the species included in the HABC analyses as possible (Table S2) and per site divergence between refugia compared between the two genes. We found no significant difference between loci in either the Iran/Balkans or Balkans/Iberia comparison (Wilcoxon signed rank test, $p = 0.79$ and 0.77 respectively). This implies that our finding of an older divergence of gallwasp hosts
 160 compared to parasitoids cannot be accounted for by different mutation rates in *cytb* and *COI*.

Supplemental References (numbered to continue from those in the main text)

45. Blum, M.G.B. and François, O. (2010). Non-linear regression models for Approximate
 165 Bayesian Computation. *Statistics and Computing*, 20, 63-73.
46. Csilléry, K., Blum, M.G.B., Gaggiotti, O.E. and François, O. (2010). Approximate Bayesian Computation (ABC) in practice. *Trends Ecol. Evol.* 25, 410-418.
47. Huang, W., Takebayashi, N., Qi, Y., Hickerson, M.J. (2011). MTML-MSBAYES –
 170 Inferring temporal biogeographic congruence across with multiple loci data. *BMC Informatics* 12, 1.
48. Hey, J. (2010). Isolation with Migration Models for More Than Two Populations. *Mol. Biol. Evol.* 27, 905-920.
49. Christian P. Robert, Jean-Marie Cornuet, Jean-Michel Marin, and Natesh S. Pillai (2011). Lack of confidence in approximate Bayesian computation model
 175 choice. *Proc. Nat. Acad. Sci. USA* 1102900108v1-6.